Analysis of Motion Response of Wind Turbine Platform Considering Different Heading Angles and Water Depths

Xingda Chen, Huimin Yu, Wei Wang and Bingyang Wang
Zhejiang Ocean University, Zhoushan, Zhejiang, 316022

***Abstract*—Due to the occurrence of the overturning of the offshore wind turbine platform, this paper has conducted in-depth research on the offshore structure response of the wind turbine. Using the SESAM software, the wind turbine model was constructed to compare the motion response and structural response of the nose to the multi-floating wind power platform at different heading angles. Secondly, the magnitude of the motion response value of the floating platform of the fan under different water depths and the stress at the joint of the pontoon rod and the change of the RAO value are compared. The results show that the motion response and heading change of the fan platform are not obvious, and the water depth has a certain influence on it, and it is more obvious in shallow water. Therefore, in the future design of multi-floating wind power generation platform, the impact of wind turbine head steering changes on the structure can be neglected, but the effect of water depth on motion response and dynamic response should be integrated and considered to ensure that the platform can be safer.**

Keywords—wind turbine; dynamic response; water depth; heading angle

I. PREFACE

Wind power has become one of the most popular new energy technologies in the world. Due to the wind energy advantages of the ocean, land-based wind turbines are gradually developing into the ocean, and from shallow to deep.The floating platform is an ideal form of deep-water turbines, which has received extensive attention from people in various countries. Successful development of a stable and safe floating platform is of great significance for the effective use of wind energy and new energy development.

Due to the large load of offshore wind and wave, it has a great impact on the safety of the floating wind turbine platform. When the platform is overturned, it is very important to study the motion response of the wind turbine under different water depths and wind waves to ensure the safe operation of the wind turbine. In this paper, the sesam software, which is the preferred marine structure analysis, is used to analyze the motion response. Considering the complexity of the marine environment, this paper simplifies the flow load, linearizes it, and applies the wind load with a constant wind field. In order to get the maximum wind energy from the wind turbine blades facing the windward side, the cabin is required to automatically turn and change the heading angle. When the nacelle is rotating, the change of heading angle will affect the overall force of the fan. It is important to analyze the impact of this effect on the stability of the fan, which is important for the stability evaluation of the fan.

Secondly, this paper refers to Tao Kai's research method of analyzing the motion response of three different floating platforms under different water depths by using finite element software. Finally, the motion response value of the fan under different water depths is obtained, and the selection of the fan platform according to the water depth is proposed. Reasonable suggestions are of great significance for the future development of floating platforms.

II. ENVIRONMENTAL LOAD

The marine environment is highly complex and requires not only wind loads but also wave loads, flow loads, and the like. Since only the overall motion response of the floating platform is considered in this paper, and the individual vibration of the fan blade is not considered. Therefore, when the wind load is applied, the pressure simulation can be performed by constructing a wind disk and applying a constant wind field.

A. Wave Load

The biggest difference between offshore and land fans is the impact of wave loads, which affect wind turbine platforms even more than wind loads. The hydrodynamic effects of wave loads on floating platforms include wave excitation and radiation forces, and wave drift forces. Among them, the wave excitation force is further divided into a periodic wave excitation force and a non-periodic wave excitation force. When the wave affects the structure, it produces a diffractive force on the surface of the structure.

In the ship design calculation, the wave method is used to directly design and calculate the structural strength of the whole ship. The floating foundation in this paper also refers to this method. The principle is to determine the main structural stress by calculating the main parameters such as the period, wave height and wavelength of the wave, so that it acts on the hull according to a certain phase and direction.

The core of the method is how to calculate the design wave that can be equivalent to the dangerous condition of the ship during navigation.

Usually, the ship is subjected to long-term prediction of the wave load in the navigational waters, and then the predicted extreme value of the main load control parameters of the hull exceeding the probability level of 10-8 is obtained, and the regular wave capable of generating the equivalent stress response with the long-term prediction is selected. This regular wave can be used as an equivalent design wave for direct calculation of the hull structural strength.

The amplitude of the equivalent design wave is the ratio of the extreme value of the long-term prediction of the main load control parameters to the maximum value of the amplitude of the transfer function, as shown in equation (1):

$$a_w = \frac{L_j}{A_j} \tag{1}$$

Where: a_w represents the amplitude of the equivalent design wave; L_j represents the long-term forecast extreme value of the main load control parameters; A_j represents the maximum amplitude of the transfer function; j represents the number of the main load control parameters.

The frequency and wave direction of the design wave correspond to the frequency and the wave direction frequency corresponding to the maximum amplitude of the main control load parameter transfer function.

The design wave parameters determined by the above method are shown in Table 1:

TABLE I. DESIGN WAVE PARAMETERS

Working condition	Main load control parameter	Wave direction(deg)	Angular frequency(rad/s)	amplitude(m)
LC1	Heave	180	0.6	8.6
LC2	Pitch	180	0.3	13.6
LC3	Yaw	150	0.1	7.1

B. Wind Load

Offshore winds are highly complex and cannot be well simulated, and wind loads cannot be analyzed in the SESAM software, so static pressure is applied to simulate a constant wind field using the interface Patran_Pre. of MSC and DNV software. Since the vibration influence of the fan blade is neglected, the fan blade is built into a disk at the time of modeling, and the calculated wind load is applied to the disk. When the fan is in the sea state of normal power generation, the average pressure of the entire disk area of the fan is:

$$P_H = \frac{1}{2}\rho C_{FB} V_r^{\,2} \tag{2}$$

Where: ρ indicates the air density, generally ρ =1.297 kg/m^3; C_{FB} is the coefficient, according to the Bates formula can be taken $C_{FB} = \frac{8}{9}$; V_r represents the wind speed. Horizontal wind load at the top of the wind turbine tower:

$$F_H = P_H A_O = P_H \frac{\pi D^2}{4} \tag{3}$$

The wind load of the tower is calculated as follows:

$$F_{to} = k_1 k_2 a v_t^{\,2} A_w \tag{4}$$

Where: k_1 is the wind load shape factor, the beam and the side wall of the building is 1.5, the side wall of the cylinder is 0.5; k_2 is wind pressure height variation coefficient; a is the wind pressure coefficient which is 0.613; v_t is the Design wind speed(m/s) with time interval t; A_w indicates the projected windward area of the tower.

The wind load on the impeller and the wind load on the tower are calculated according to equations (3) and (4) respectively. If we substitute the correlation coefficient into it, we can obtain equation (5).

$$p_H = \frac{V_r^{\,2}}{1800} \tag{5}$$

The height coefficient in formula (4) can be taken as shown in Table 2.

TABLE II. HEIGHT COEFFICIENT k_2

Height above sea level z(m)	Height factor	Height above sea level z(m)	Height factor	Height above sea level z(m)	Height factor
0-2	0.64	20-30	1.29	70-80	1.58
2-5	0.84	30-40	1.37	80-90	1.62
5-10	1.00	40-50	1.43	90-100	1.64
10-15	1.11	50-60	1.49	100-150	1.79
15-20	1.18	60-70	1.54	150-200	1.90

C. *Current Load Setting*

In this chapter, the current load calculation uses the random method to linearize the drag force. Based on the most likely maximum motion response estimation linearization matrix of the hypothetical Rayleigh distribution, the force and damping are updated according to this matrix. The Morrison drag force linearization coefficient matrix is calculated by an iterative method.

III. CALCULATION MODEL

The wind turbine platform studied in this paper uses GeniE modeling in SESAM software and uses HydroD software for calculation. In the calculation, three calculation models were used: the wet surface model was used to calculate the stability of the structure, the Morrison model was used to calculate the wave force, and the mass model was used to specify the mass. The models are shown in Figures 1 to 3:

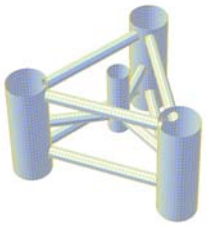

FIGURE I. WET SURFACE MODEL

FIGURE II. STRUCTURAL MODEL

FIGURE III. QUALITY MODEL

FIGURE IV. BALLAST COMPARTMENT LAYOUT

In this calculation, the method of adjusting ballast is used to balance the buoyancy and gravity. Each ballast chamber is provided with a plurality of ballast chambers, which are filled with different ballasts. The ballast tanks in this paper are arranged as shown in Figure 4.

IV. CALCULATION RESULTS

A. *Motion Response Results at Different Heading Angles*

The selected sea conditions are the rated working sea conditions of the wind turbine. The wind speed is 8 m/s, the wave spectrum is JONSWAP spectrum, the significant wave height is 10 m, the wave period is 12.0 s, and the water depth is 200 m. Since the floating platform of the model arranges the pontoon on the apex of the equilateral triangle, the dynamic response and structural response to the structure are equivalent when the fan cross section changes by every 60º. Five different angles were set in range of 60º: 0º, 15º, 30º, 45º, 60º to study the calculation.

After the HydroD module of the SESAM software is calculated, the calculation data is read using the post-processing program POSTRESP, and the motion response in six degrees of freedom and the structural response result of the structure are obtained. When the heading angle is 0 degrees, the rolling angle, the pitching angle and the yawing

angle are all within 10 degrees, and the floating fan is in a normal working state. Therefore, taking the 0 degree sailing angle as a reference, compare the changes under different angles, and calculate the statistical results as shown in Table 3:

TABLE III. STATISTICAL RESULTS OF MOTION RESPONSE IN DIFFERENT HEADING ANGLES

Sailing angle	Wave direction	Surging	Swaying	Heaving	Rolling	Pitching	Yawing
0	150	1.326	0.785	3.389	0.0055	0.0056	0.011
	180	1.512	0	3.426	0	0.0081	0
15	150	1.325	0.785	3.389	0.0056	0.0057	0.012
	180	1.512	0	3.426	0.0001	0.008	0
30	150	1.326	0.788	3.389	0.0056	0.0055	0.011
	180	1.514	0	3.426	0.0002	0.0079	0
45	150	1.326	0.785	3.388	0.0057	0.0054	0.011
	180	1.513	0	3.426	0.0003	0.0078	0
60	150	1.325	0.786	3.389	0.0057	0.0054	0.011
	180	1.512	0	3.425	0.0004	0.0076	0.001

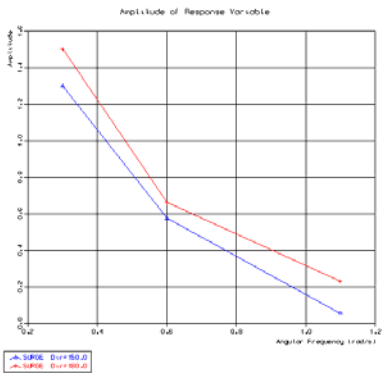

a. surging

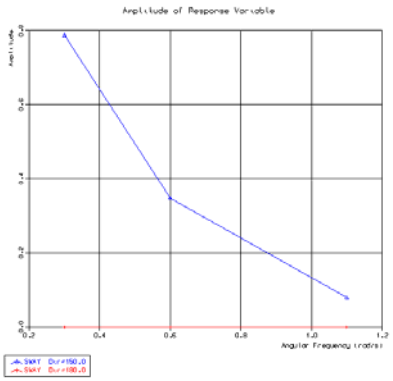

b. swaying

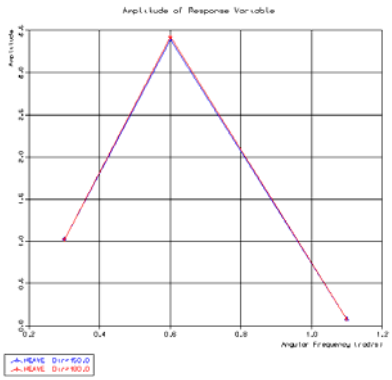

c. heaving

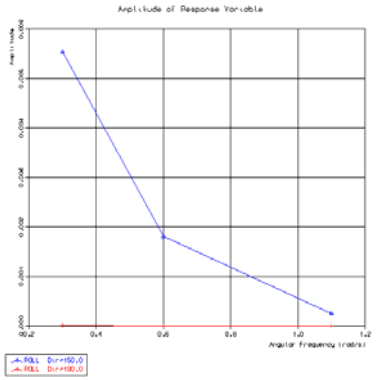

d. rolling angle

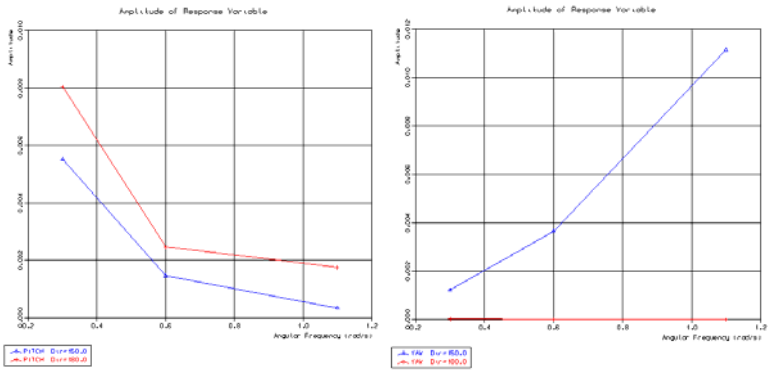

e. pitching angle f. yawing angle

FIGURE V. 6-DEGREE-OF-FREEDOM MOTION RESPONSE

It can be seen from Table 3 that different heading angles have a significant influence on the rolling and pitching of the multi-floating wind power platform. The relationship between the RAO value change of other degrees of freedom motion response and the heading change is not obvious.

It can be seen from the motion response Figure 5 that under different degrees of freedom, the RAO changes with the angular frequency, and the motion response in the surging, swaying, rolling, and pitching decreases as the angular frequency increases; the maximum value of the motion response during heaving is 3.426; it increases with the increase of the angular frequency during the yawing.

Stress analysis is carried out on the structural response results of the five headings. Using the Sestra module in the SESAM software, this paper only considers the floating foundation mechanism. According to the results, the stresses of different heading angle structures do not change much, as shown in Table 4.

TABLE IV. STATISTICAL RESULTS OF DIFFERENT HEADING ANGLE STRESSES

sailing angle	0°	15°	30°	45°	60°
Maximum stress	2.4420E+08	2.4337E+08	2.4337E+08	2.4426E+08	2.4469E+08

B. Motion Response Results at Different Water Depths

In view of the fact that previous researchers have set the water depth to 50m or more, and the water depth within 50m has not been considered, this paper will study the water depth within 50m, a series with a difference of 5m, one of which is set to the characteristic length. . The water depth series considered in this paper are: 27m, 32m, 37m, 42m, 47m.

When the fan platform is set at five water depths, the calculated data is read from the POSTRESP to obtain a motion response at six degrees of freedom. According to the comparison of the graphs, the fan will peak under the action of waves with a heaving of 0.3 to 1.1 rad/s under five water depths. The other degrees of freedom motion response in this interval are the highest value at the interval boundary and the peak value decreases as the water depth increases. The peak value under the heaving is as shown in Figure 6.

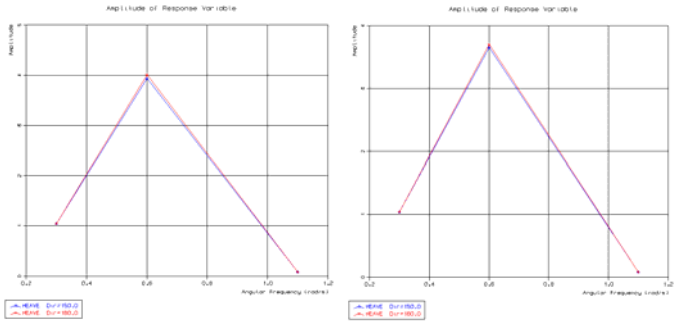

a. 27m heaving b. 32m heaving

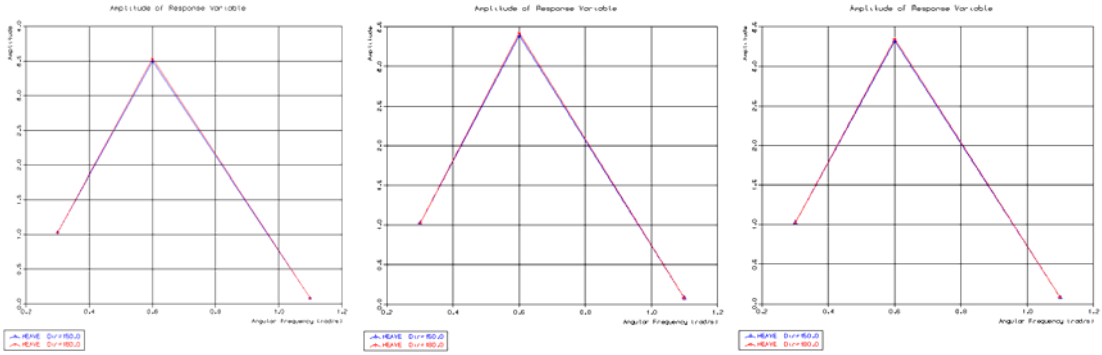

c. 37m heaving d. 42m heaving e. 47m heaving

FIGURE VI. MOTION RESPONSE OF EACH WATER DEPTH

It can be seen from the above Figure 6 that when the water depth is 27m, 32m, 37m, 42m, 47m, the RAO values reach a peak under the action of 0.6rad/s, and the corresponding values are respectively 4.006, 3.703, 3.535, 3.426, 3.351, obviously, the peak value of the RAO value gradually decreases as the water depth increases.

C. Study on the Influence of Different Water Depths on the Stress at the Two Ends of the Main Buoy Connecting Rod

On this basis, two nodes are selected for analysis between the connecting rods of the floating platform connecting the pontoons, and the stress values of some plate units near the connecting points at different water depths are tracked. The serial number definition of the components is shown in Figure 7. Under different water depths, the joint stress changes are different. The structural response of the joints at the connecting rods 1, 2 and 3 increases with the increase of water depth. The stress at the connecting rods 4, 5 and 6 varies with the water depth, and an extreme value occurs, which then tends to stabilize.

It can be seen from Figure 8 that the structural response maximum curve of the structure changes significantly, which indicates that the water depth has a significant influence on the maximum value of the structural response. When the water depth is less than 32m, the curve decreases with the increase of water depth, and slows down faster, that is, the smaller the water depth, the larger the structural response maximum. When the water depth is between 32m and 47m, the maximum structural response tends to be stable and does not decrease or increase, indicating that when the water depth reaches a certain depth, the structural response does not change with the increase of water depth.

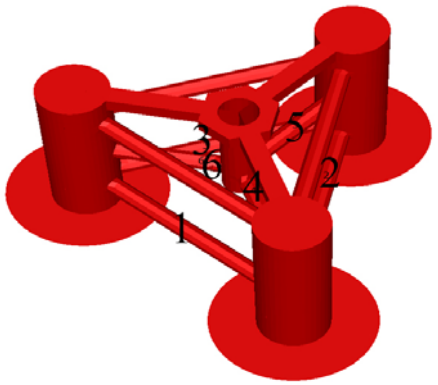

FIGURE VII. ARRANGEMENT OF THE ROD NUMBER FIGURE

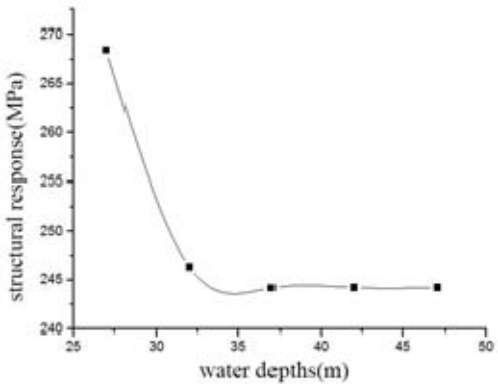

FIGURE VIII. MAXIMUM STRUCTURAL RESPONSE AT DIFFERENT WATER DEPTHS

V. CONCLUSION

In this paper, the influence of different heading angles on the fan is analyzed. The RAO value changes with the angular frequency under the six degrees of freedom. The difference between the different heading angles is compared. The Stress response diagrams under different angles is obtained by analysis. At the same time, the influence of water depth on the fan is also considered, and the motion response and

structural response at different water depths are calculated. The results show that:

(1) Under different heading angles, the variation of RAO value is basically the same, and it has little relationship with the change of heading angle. When the heading angle changes, the RAO value has a significant influence on the rolling and pitching of the multi-floating wind power platform, and the change of the motion response to other degrees of freedom is not obvious. Therefore, the design of the fan should focus on the anti-rolling of these two situations.

(2) The water depth has a certain influence on the response of the fan. As the water depth deepens, the amplitude of the fan power generation platform is generally reduced under various degrees of freedom. And the effect of setting the fan platform at the deeper water depth is better; When the water depth becomes shallow, the maximum structural response of the fan is almost constant, but when a certain value is reached (this value may be the characteristic value), the change becomes very obvious, and increases rapidly as the water depth becomes shallower;

(3) When the water depth and the environmental load are the same, by analyzing the stress cloud map, it can be found that the change of different angles has little effect on the stress of the fan. Therefore, in the relevant numerical simulation of the wind turbine, it can simplify the stress effect of the change of the wind turbine nose steering on the structure.

(4) The motion response and structural response of the wind turbine are related to the water depth. The water depth should be taken into account when designing the wind turbine. This will put forward higher requirements for the development of the future wind turbine platform to ensure that the wind turbine platform can be safer.

REFERENCES

[1] Su Xiao. Statistics and Analysis of Global Offshore Wind Power Development in 2012 [J]. Wind Energy, 2013, (6).

[2] Liu Zhongbai, Tang Yougang, Wang Han, et al. Experimental study on the characteristics of semi-submersible wind power floating foundation[J]. Journal of Harbin Engineering University, 2015(1).

[3] DUARTE T, GUEYDON S, JONKMAN J, SARMENTO A. Computation of wave loads under multidirectional sea states for floating offshore wind turbines[C]// Proceedings of the 33rd International Conference on Ocean, Offshore and Arctic Engineering-OMAE2014.San Francisco, California, USA, ASME, 2014.

[4] Li Yan. Research on basic design of single-point mooring floating wind turbine[A]. China Ocean Engineering Society. Proceedings of the 17th China Ocean (Ashore) Engineering Symposium (I) [C]. China Ocean Engineering Society: 2015: 8.

[5] DUAN L, KAJIWARA H.A coupled aero hydrodynamic simulator for offshore floating wind turbines [C]// Proceedings of the 33rd International Conference on Ocean, Offshore and Arctic Engineering OMAE2014, San Francisco, California, USA, ASME, 2014.

[6] Wang Ning. Overall performance analysis of offshore buoyancy wind turbine platform [D]. Harbin Engineering University, 2013.

[7] M. Salman Siddiqui, Adil Rasheed, Trond Kvamsdal, Mandar Tabib. Quasi-Static & Dynamic Numerical Modeling of Full Scale NREL 5MW Wind Turbine [J]. Energy Procedia, 2017, 137.

[8] Cao Jun, Tang Yougang, Tao Haicheng, et al. Study on floating foundation design and amplitude-frequency motion characteristics of semi-submersible fans[J]. Ocean Engineering, 2013, 31(2): 61-67.

[9] Zhang Shaoheng. Comparison of Daveport wind speed spectrum and Kaimal wind speed spectrum in communication tower design[J]. Special Structure,2012(4).

[10] Wu Songren. Coastal Dynamics [M]. Beijing: China Communications Press, 2004: 8-44.

[11] Yu Xiaochuan, Xie Yonghe, Li Runpei et al. Effect of water depth on motion response and wave loading of super large FPSO [J].

[12] HydorD USER MANUAL.DNV Software Report, No: 2004-0199/Revision4, 2008.

[13] Tao Kai. Dynamic response of deep-water floating wind turbines [D]. Jiangsu University of Science and Technology, 2014.